Accepted article of: M. Morawiec, K. Blecharz and A. Lewicki, "Non-Adaptive Speed and Position Observer of Doubly-Fed Induction Generator," 2022 International Conference on Electrical Machines (ICEM), 2022, pp. 1744-1749, doi: 10.1109/ICEM51905.2022.9910788.

Non-Adaptive Speed and Position Observer of Doubly-Fed Induction Generator

M. Morawiec, K. Blecharz, Arkadiusz Lewicki

***Abstract* – The non-adaptive speed and position estimation of a doubly-fed induction generator (DFIG) is presented in this paper. The speed observer is based on the mathematical model of DFIG and to stabilize the structure the Lyapunov method is used. The classic stator field-oriented control to active and reactive power control is used in the sensorless control system. The performance of the proposed algorithm of a speed observer is validated by simulation and experimental results using the 2 kW generator. The stability analysis of the presented solution is confirmed by using the Lyapunov method and practical stability theorems.**

***Index Terms*—Doubly fed induction generator (DFIG), sensorless control, state observer.**

I. NOMENCLATURE

$i_{sx,y}$	stator current vector components,
$i_{rx,y}$	stator current vector components,
$u_{r\alpha,\beta}$	rotor voltage vector components,
$u_{s\alpha,\beta}$	stator voltage vector components,
ω_r	rotor angular speed,
θ_r	rotor position,
R_r, R_s	rotor and stator resistances,
L_m	mutual-flux inductance,
L_s, L_r	stator and rotor inductances,
T_e	electromagnetic torque,
T_L	load torque,
J	machine torque of inertia,
τ	relative time,
$\hat{\theta}_r$	estimated rotor position,
$\hat{\omega}_r$	estimated rotor electrical speed,
$\tilde{\omega}_r$	rotor speed error,
$\tilde{\theta}_r$	rotor position error,
"^"	estimated values,
"~"	error of estimated values,
(x, y)	coordinate system is associated with any angular speed.

II. INTRODUCTION

The rotor speed and position estimation are widely studied in the literature. These methods can be divided into two main groups: the open-loop and the close-loop. In the open-loop position estimators, the rotor currents are measured and processed in different reference frames. The value of the rotor position is calculated by comparing the components of the current [1]-[4]. The second group is the close-loop estimators based on the different models of the full or reduced-order observers. In addition to classic solutions such as nonlinear full order observers [5]–[6], extended Luenberger observers [7], extended Kalman filters [8], MRAS [9]–[10] there exist the methods of observers or controls named "robust". The group of robust estimators includes: based on backstepping [11], the interconnected observers [12], and above all based on the sliding-mode techniques [13]. A large group of solutions are algorithms based on the model reference adaptive system (MRAS) approach [9]-[10], [14]. The algorithm of MRAS can be realized in different variations when the selected state variable is specified in stator or rotor co-ordinates. The rotor position is determined by using the adaptive law.

In the literature [1]-[14] the various control methods are proposed. The most popular methods are based on the stator flux orientation and is named field-oriented control (FOC) [6], [10]-[11]. Alternative to FOC is the direct power control proposed in [15]. The nonlinear control approaches have also been used in the DFIG system, such as feedback linearization via the backstepping [16] and sliding mode control [18]. The circuit (windings) of the DFIG generator can be modeled by using the approach presented in [19].

In this paper there is proposed the observer structure which is based on the DFIG mathematical model [11], however, the values of rotor speed and rotor position are not obtained by using the adaptive law but the non-adaptive approach. The rotor position is calculated by using the introduced to observer internal variables. The rotor position can be determined by using the simple integrator structure and additional stabilizing law. The proposed solution was validated by using the simulation and in the experimental setup with the 2 kW DFIG connected to the rotor side by the voltage source converter and to the AC-grid by the stator side. The classical FOC control structure is used to control the active and reactive stator powers. The properties of the FOC control system of DFIG are presented.

III. MATHEMATICAL MODEL OF DIFG

The mathematical model of DFIG can be determined in the stationary reference frame or rotating frame by the differential

M. Morawiec is with Gdansk University of Technology, Faculty of Electrical and Control Engineering, Department of Electric Drives and Energy Conversion – (email: marcin.morawiec@pg.edu.pl)

K. Blecharz is with Gdansk University of Technology, Faculty of Electrical and Control Engineering, Department of Electric Drives and Energy Conversion – (email: krzysztof.blecharz@pg.edu.pl)

A. Lewicki is with Gdansk University of Technology, Faculty of Electrical and Control Engineering, Department of Electric Drives and Energy Conversion – (email: arkadiusz.lewicki@pg.edu.pl)

equations for the rotor and stator current vector components

$$\frac{di_{sx}}{d\tau}=-\frac{L_s}{w_\sigma}(R_s i_{sx}-u_{sx})+\frac{L_m}{w_\sigma}\left(\omega_r(L_m i_{sy}+L_r i_{ry})+R_r i_{rx}-u_{rx}\right), \quad (1)$$

$$\frac{di_{sy}}{d\tau}=-\frac{L_r}{w_\sigma}(R_s i_{sy}-u_{sy})-\frac{L_m}{w_\sigma}\left(\omega_r(L_m i_{sx}+L_R i_{rx})-R_r i_{ry}+u_{ry}\right), \quad (2)$$

$$\frac{di_{rx}}{d\tau}=\frac{L_s}{w_\sigma}\left(-\omega_r(L_r i_{ry}+L_m i_{sy})-R_r i_{rx}+u_{rx}\right)+\frac{L_m}{w_\sigma}\left(R_s i_{sx}-u_{sx}\right), \quad (3)$$

$$\frac{di_{ry}}{d\tau}=\frac{L_s}{w_\sigma}\left(\omega_r(L_r i_{rx}+L_m i_{sx})-R_r i_{ry}+u_{ry}\right)+\frac{L_m}{w_\sigma}(R_s i_{sy}-u_{sy}), \quad (4)$$

$$\frac{d\omega_r}{d\tau}=\frac{L_m}{JL_r}\left(i_{rx}i_{sy}-i_{ry}i_{sx}\right)-\frac{1}{J}(T_L+f_r\omega_r). \quad (5)$$

where (x, y) coordinate system is associated with any angular speed and it is assumed that (1)–(2) are connected to the stationary stator windings so the angular speed of the (x,y) system is $\omega_a=0$, f_r is the friction.

In the theoretical investigations, it is assumed that all the DFIG parameters are known and constant, the rotor speed is estimated by the observer structure. In the FOC control system u_{rx}, u_{ry} are treated as the control vector variables and u_{sx}, u_{sy}, i_{sx}, i_{sy} and i_{rx}, i_{ry} components are treated as measured and transformed to the adequate (x, y) reference frame.

IV. Speed Observer Structure of DFIG

Considering the mathematical model dependences (1)–(4) the observer structure for the DFIG can be obtained similar to [11] for the rotor current vector components and for the introduced to the structure new variables marked as $H_{x,y}$:

$$\frac{d\hat{i}_{rx}}{d\tau}=-\frac{L_s}{w_\sigma}(\hat{H}_y+R_r i_{rx}+u_{rx})+\frac{L_m}{w_\sigma}(R_s i_{sx}-u_{sx})+v_{rx}, \quad (6)$$

$$\frac{d\hat{i}_{ry}}{d\tau}=\frac{L_S}{w_\sigma}(\hat{H}_x-R_r i_{ry}+u_{ry})+\frac{L_m}{w_\sigma}(R_s i_{sy}-u_{sy})+v_{ry}, \quad (7)$$

$$\frac{d\hat{H}_x}{d\tau}=\hat{\omega}_r(-\hat{H}_y-R_r i_{rx}+u_{rx})+v_{Hx}, \quad (8)$$

$$\frac{d\hat{H}_y}{d\tau}=\hat{\omega}_r(\hat{H}_x-R_r i_{ry}+u_{ry})+v_{Hy}, \quad (9)$$

$$\frac{d\hat{\theta}_r}{d\tau}=\hat{\omega}_r+v_\theta, \quad (10)$$

where estimated state variables are marked by "^" and $\frac{d\hat{\omega}_r}{d\tau}\approx\frac{\Delta\hat{\omega}_r}{\Delta T}$ and

$$H_x=\omega_r(L_m i_{sx}+L_r i_{rx}), \quad (11)$$

$$H_y=\omega_r(L_m i_{sy}+L_r i_{ry}). \quad (12)$$

The observer structure contains the following stabilization functions v_{rx}, v_{ry} and v_{Hx}, v_{Hy}, v_θ which can be obtained by using design procedure based on the Lyapunov theorem.

The first step of the proposed procedure is to determine the deviations model of the structure (6)–(10). Considering (3)–(4) and (6)–(9) as well as (11)–(12), denoting the estimation errors by "~", one can obtain

$$\frac{d\tilde{i}_{rx}}{d\tau}=-\frac{L_s}{w_\sigma}\tilde{H}_y+v_{rx}, \quad (13)$$

$$\frac{d\tilde{i}_{ry}}{d\tau}=\frac{L_s}{w_\sigma}\tilde{H}_x+v_{ry}, \quad (14)$$

$$\frac{d\tilde{H}_x}{d\tau}=\hat{\omega}_r(-\tilde{H}_y+R_r\tilde{i}_{rx})+v_{Hx}, \quad (15)$$

$$\frac{d\tilde{H}_y}{d\tau}=\hat{\omega}_r(\tilde{H}_x-R_r\tilde{i}_{ry})+v_{Hy}, \quad (16)$$

$$\frac{d\tilde{\theta}_r}{d\tau}=\tilde{\omega}_r+v_\theta, \quad (17)$$

where

$$\tilde{i}_{rx}=\hat{i}_{rx}-i_{rx}, \tilde{i}_{ry}=\hat{i}_{ry}-i_{ry}, \ \tilde{H}_x=\hat{H}_x-H_x, \tilde{H}_y=\hat{H}_y-H_y. \quad (18)$$

The next step of the procedure is to stabilize the structure (6)–(10) through the introduced functions v_{rx}, v_{ry} and v_{Hx}, v_{Hy}. The Lyapunov function for the observer system deviations is proposed

$$V=\frac{1}{2}(\tilde{i}_{rx}^2+\tilde{i}_{ry}^2+\tilde{H}_x^2+\tilde{H}_y^2+\tilde{\theta}_r^2)>0, \quad (19)$$

and must be positively determined.

The derivatives of the Lyapunov function is

$$\dot{V}=-c_x\tilde{i}_{rx}^2-c_y\tilde{i}_{ry}^2+\tilde{i}_{rx}\left(c_x\tilde{i}_{rx}+v_{rx}\right)+\left(c_y\tilde{i}_{ry}+v_{ry}\right)+ +\tilde{H}_x\left(\hat{\omega}_r R_r\tilde{i}_{rx}+\frac{L_s}{w_\sigma}\tilde{i}_{ry}+v_{Hx}\right)+\tilde{H}_y\left(-\hat{\omega}_r R_r\tilde{i}_{ry}-\frac{L_s}{w_\sigma}\tilde{i}_{rx}+v_{Hy}\right). \quad (20)$$

The proposed observer structure will be asymptotically stable if $\dot{V}_2<0$ and if the stabilizing functions introduced to the structure are determined

$$v_{rx}=-c_x\tilde{i}_{rx}, \quad (21)$$

$$v_{ry}=-c_y\tilde{i}_{ry}, \quad (22)$$

$$v_{Hx}=c_{Hx}(-\frac{L_s}{w_\sigma}\tilde{i}_{ry}-\hat{\omega}_r R_r\tilde{i}_{rx}), \quad (23)$$

$$v_{Hy}=c_{Hy}(\frac{L_s}{w_\sigma}\tilde{i}_{rx}+\hat{\omega}_r R_r\tilde{i}_{ry}), \quad (24)$$

where (c_x, c_y, c_{Hx}, c_{Hy}, c_θ) > 0 are the observer tuning gains and

$$v_\theta=-c_\theta\tilde{\theta}_r. \quad (25)$$

The speed observer structure will be asymptotically stable if (21)–(25) is satisfied. In the sensorless control, the rotor speed is not measured therefore the deviation $\tilde{\theta}_r$ in (25) should be replaced by $\tilde{\theta}_H$, which means the deviation between the estimated values of H_x and H_y, calculated from (11)–(12) and estimated from the observer structure by using (8)–(9) as follows [11]

$$\tilde{\theta}_H=\tan^{-1}(\vartheta), \quad (26)$$

where $\vartheta=\frac{H_x\hat{H}_y-H_y\hat{H}_x}{H_x\hat{H}_x+H_y\hat{H}_y}$ and $(H_x\hat{H}_x+H_y\hat{H}_y)\neq 0$. (27)

For (c_x, c_y, c_{Hx}, c_{Hy}, c_θ) > 0, it can be proved that the estimation errors defined in (18) are decayed to zero in finite time and the estimation values are converged to their real values. It means that the derivative of Lyapunov function is $\dot{V}\le-\mu\sqrt{V}, \mu=\sqrt{2}\delta_\theta$ for $\delta_\theta>0$ and the values of errors (18) are bounded. By virtue of the theorem presented in [12] the speed observer structure is practically stable. Considering (11) –(12) and after some calculations, the rotor speed can be estimated from the following dependence

$$\hat{\omega}_r = \frac{\hat{H}_x \hat{\psi}_{rx} + \hat{H}_y \hat{\psi}_{ry} - c_f (\hat{H}_x \hat{\psi}_{ry} - \hat{H}_y \hat{\psi}_{rx})}{\hat{\psi}_{rx}^2 + \hat{\psi}_{ry}^2}, \tag{28}$$

where

$$\hat{\psi}_{rx} = L_m i_{sx} + L_r \hat{i}_{rx}, \tag{29}$$

$$\hat{\psi}_{ry} = L_m i_{sy} + L_r \hat{i}_{ry}, \tag{30}$$

$c_f \geq 0$ and $(\hat{\psi}_{rx}^2 + \hat{\psi}_{ry}^2) \neq 0$.

The tuning gains in the experimental stand are chosen: $c_x = c_y = 10$, $c_{Hx} = c_{Hy} = 5$ p.u., $c_\theta = 0.1$ and $c_f = 15$ p.u.

The control system structure is presented in Fig. 8. There is the classical FOC presented in [1-4]. In the next section, the theoretical dependences are confirmed by using simulation and experimental research.

V. Simulation Results

The simulation model of the DFIG system contains the doubly-fed machine model, wind emulators, and the VSI model with the space vector modulation (SVM). The sample period for the control system is 150 μs and for the SVM is 300 μs. The system parameters are presented in Table 1.

In Fig. 1 the active power (s_p) is changed from -0.1 to -0.35 after 100 ms (reactive power (s_q) is set to -0.6) and after 400 ms the active and reactive powers are changed together - s_p to 0.35, s_q to 0.2 p.u. The estimation error of rotor speed is smaller than 0.01 in the steady-state and about 0.015 in the transient state. The rotor position error is about 0.012 in the steady-state and about 0.017 in the transient state. The rotor current components i_{rd}, i_{rq} are shown.

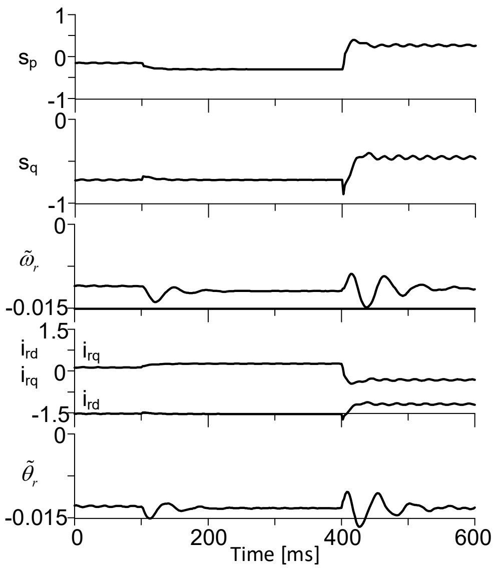

Fig. 1. Active and reactive power changes

In Fig. 2 the active power s_p is set to 0.02 p.u. and reactive power s_q is set to -0.6 p.u. The rotor speed of the DFIG is changed from the sub-synchronous to super-synchronous mode. During the rotor speed crossing through the synchronous speed (1.0 p.u.) the estimated speed error is increased. The error of rotor position is almost constant and about 0.01 p.u.

In Fig. 3 the estimation error of rotor current vector components, rotor flux vector component (connected to stator), estimated $\hat{\theta}_r$ and measured θ_{rM} rotor position, rotor position error $\tilde{\theta}_r$, estimated rotor current vector components in the steady-state. The stator active power is set to -0.35 p.u. and the stator reactive power is -0.6 p.u.

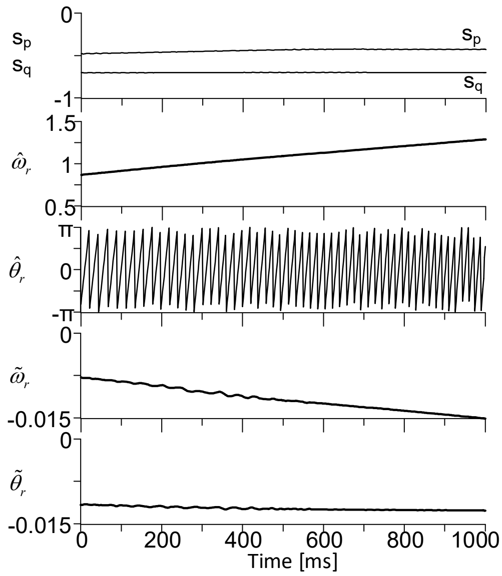

Fig. 2. Crossing from sub-synchronous to super-synchronous working mode

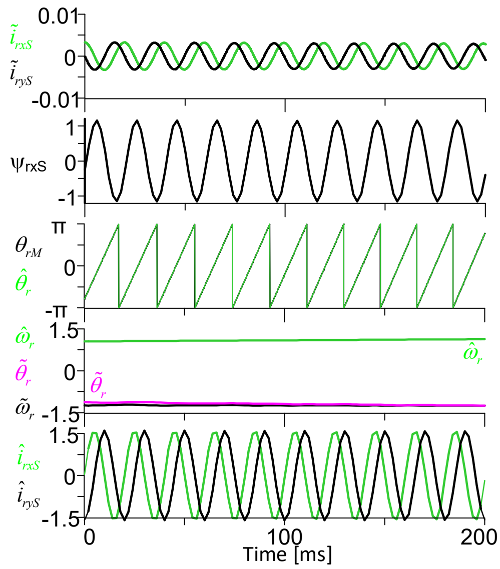

Fig. 3. Estimated variables from the speed observer in steady-state and their errors (sub-synchronous) – index "S" means connected to the stator

The simulation results confirm that the speed observer structure reconstructs the estimated rotor position and rotor speed with small errors and the structure is stable even crossing through the synchronous rotor speed. In the next the experimental results are presented.

VI. EXPERIMENTAL RESULTS

Experimental results were carried out in a 2 kW generator system (Table I in Appendix). The control system was implemented in a digital signal processing driver board with a Sharc ADSP21363 floating-point signal processor and Altera Cyclone II FPGA. The PWM switching frequency was 6.6 kHz. The code of the algorithm was not optimized for a DSP processor. The experimental stand contains the DFM connected to the squire cage induction machine. The stator of DFM was supplied to the AC grid. The rotor was connected to the AC-grid through the VSC [17].

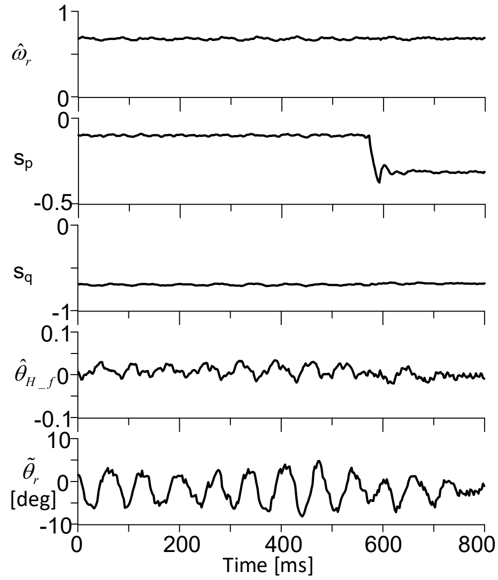

Fig. 4. Rotor speed and error of a rotor angle position in response to a step from -0.1 to -0.35 of stator active power, reactive power set to -0.7 p.u., $\tilde{\theta}_{H\_f}$ is the filtrated value of (26)

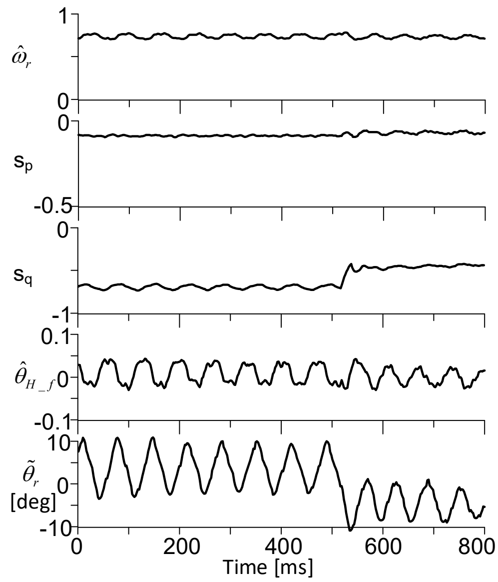

Fig. 5. Rotor speed and error of a rotor angle position in response to a step from -0.7 to -0.4 of stator reactive power, active power set to -0,1.

Fig. 4 and 5 show the observer's algorithm response to the change of the generator operating point.

In the first case, a step change of the set active power was forced. However, in the second one, the value of the magnetizing component of the stator current was changed by setting the value of the reactive power from -0.7 to a value equal -0.4 p.u. In both cases, shown in Fig. 4 and 5, in the time waveforms of the error of the rotor position error estimation $\tilde{\theta}_r$, there are visible oscillations, the amplitude of which depends on the value and character of the set reference reactive power.

Increasing the active power load of the generator has a positive effect on the performance of the speed observer whose estimation error does not exceed 5 degrees.

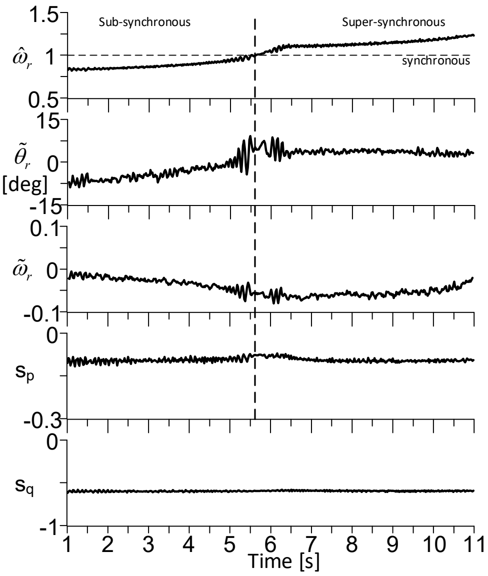

Fig. 6. Characteristic speed observer waveforms for the crossing of generator rotor speed through synchronous speed.

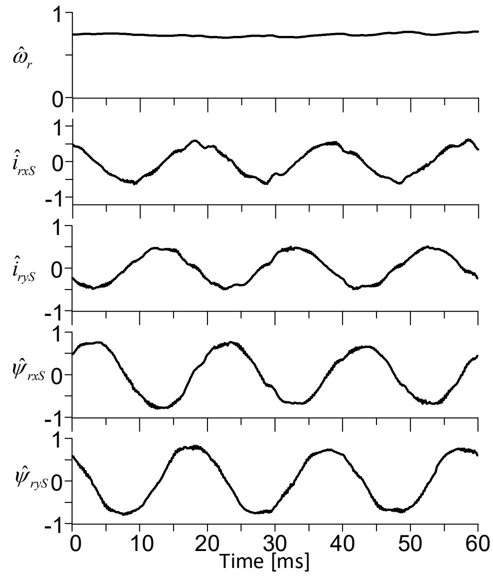

Fig. 7. The waveforms of the observer state variables for steady-state of the generator, active power set to -0.1, and reactive power set to -0.6.

In Fig. 6, the rotation speed of the generator rotor increases from 0.7 to 1.25 as a result of increasing the external driving torque of the generator. The generator power control system works correctly, the values of active and reactive power set in the control system are kept almost constant around reference values. The time waveforms presented in Fig. 6 refer to the unfavorable operating point with an underloaded generator.

Fig. 7 shows the time waveforms of the estimated rotor speed as well as the components of the rotor current vector and the rotor flux vector in a stationary reference frame with respect to the stator in the steady-state of the system.

VII. Conclusion

In the article, the algorithm of the speed observer and rotor position with a non-adaptive approach was presented. Validation of observer performance by simulation and experimental investigation was realized on a classic stator field-oriented control system. Errors in the estimation of the speed and angle of the rotor position depend on the values of active and reactive power set in the control system. The generator load with active power reduces the errors of the reproduced rotor speed and position angle, while the value and nature of the reactive power affect the oscillation amplitude of these errors. On the presented experimental results, the error of reproducing the rotor position angle in the worst case did not exceed 10-12 degrees, while in the case of a nominal loaded machine, its value oscillated below 5 degrees.
The robustness on uncertainties of nominal parameters as well as influence the tuning gains observer structure stability are not considered in this paper and these will be studied in the future.

VIII. Appendix

The control system structure with the proposed speed observer is presented in Fig. 8.

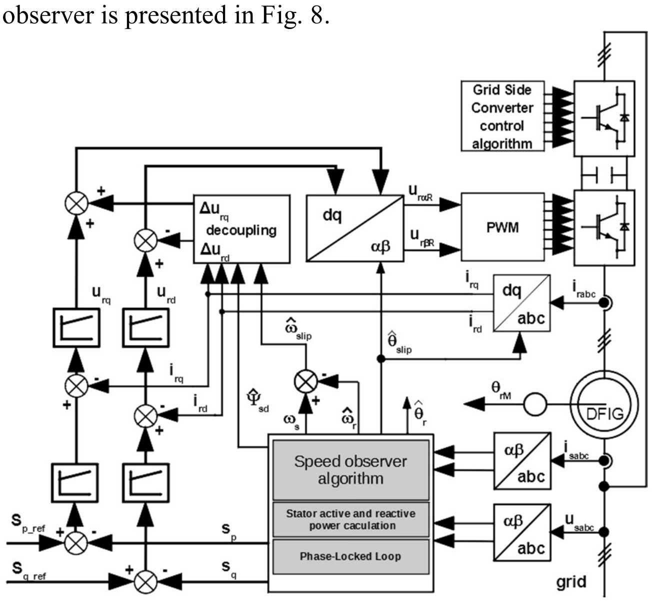

Fig. 8. The vector control structure for rotor side converter

The DFIG nominal parameters are presented in Table I.

TABLE I
DFIG Parameters and Reference Unit

Symbol	Quantity	Values
R_{sN}	stator resistance	2.833 Ω/ 0.067 p.u.
R_{rN}	rotor resistance,	2.867 Ω/ 0.068 p.u.
L_{mN}	magnetizing inductance	0.15 H/ 1.123 p.u.
L_{sN}, L_{rN}	stator and rotor inductance	0.164 H/ 1.1227 p.u
L_σ	leakage inductance	0.014 H/
P_n	nominal power	2 kW
I_{ns}	nominal stator current	5.5 A
I_{nr}	nominal rotor current	3.4 A
U_n	nominal stator voltage	400 V
N	nominal rotor speed	910 rpm
f_n	nominal frequency	50 Hz
r	Turn ratio N_s/N_r	1
$U_b=U_n$	reference voltage	400 V
$I_b=\sqrt{3}I_{ns}$	reference current	9.52 A
S_b	reference power	3810 VA

IX. References

[1] J G. D. Marques, D. M. Sousa, M. F. Iacchetti, "An Open-Loop Sensorless Slip Position Estimator of a DFIM Based on Air-gap Active Power Calculations—Sensitivity Study," *IEEE Transactions on Energy Conversion*, 28 (4), 959–968 *DOI*: 10.1109/TEC.2013.2275232.

[2] A. Karthikeyan, C. Nagamani, A. B. Ray Chaudhury, G. S. Ilango, "Implicit position and speed estimation algorithm without the flux computation for the rotor side control of doubly-fed induction motor drive," *IET Electric Power Applications*, vol. 6(4), 243–252, 2011. DOI: 10.1049/iet-epa.2010.0286.

[3] R. Bhattarai, N. Gurung, S. Ghosh and S. Kamalasadan, "Parametrically Robust Dynamic Speed Estimation Based Control for Doubly Fed Induction Generator," *IEEE Trans. on Industry Applications*, vol. 54 (6), pp. 6529-6542, Nov.-Dec. 2018, DOI 10.1109/TIA.2018.2862643.

[4] G. D Marques, D. M. Sousa, "Sensorless direct slip position estimator of a DFIM based on the air gap pq vector-sensitivity study", *IEEE Trans. on Ind. Electron.*, vol. 60(6), 2442–2450, 2012. DOI: 10.1109/TIE.2012.2218556.

[5] F. Castelli-Dezza, M. F. Iacchetti, R. Perini, "An Observer for Sensorless DFIM Drives Based on the Natural Fifth Harmonic of the Line Voltage, Without Stator Current Measurement," *IEEE Trans. on Ind. Electron.*, vol. 60(10), 4301–4309. *DOI: 10.1109/TIE.2012.2209614.*

[6] S. Yang, V. Ajjarapu, "A Speed-Adaptive Reduced-Order Observer for Sensorless Vector Control of Doubly Fed Induction Generator-Based Variable-Speed Wind Turbines," *IEEE Trans. on Energy Conf.,* 25(3), 891–900, 2010. DOI: 10.1109/TEC.2009.2032589.

[7] J. You, W. Wu, Y. Wang, "An Adaptive Luenberger Observer for Speed-Sensorless Estimation of Induction Machines", *Ann. American Cont. Conf. (ACC)*, 2018.

[8] Z. Yin, G. Li, Y. Zhang, J. Liu, "Symmetric-Strong-Tracking-Extended-Kalman-Filter-Based Sensorless Control of Induction Motor Drives for Modeling Error Reduction", *IEEE Trans. on Ind. Inf.*, vol.: 15, Iss.: 2, 2019.

[9] M. Pattnaik and D. Kastha, "Adaptive Speed Observer for a Stand-Alone Doubly Fed Induction Generator Feeding Nonlinear and Unbalanced Loads," *IEEE Transactions on Energy Conversion*, vol. 27, no. 4, pp. 1018-1026, Dec. 2012. DOI: 10.1109/TEC.2012.2217343

[10] G. D. Marques, D. M.Sousa, "New sensorless rotor position estimator of a DFIG based on torque calculations-stability study," *IEEE Transactions on Energy Conversion*, vol. 27(1), 196–203, 2012. DOI: 10.1109/TEC.2011.2174441

[11] M. Morawiec, K. Blecharz, A. Lewicki "Sensorless rotor position estimation of doubly fed induction generator based on backstepping technique*", IEEE Trans. on Ind. Electron.*, Vol. 67, Issue: 7, pp. 5889-5899, 2020.

[12] M. A. Hamida, J. De Leon, A. Glumineau, R. Boisliveau, "An Adaptive Interconnected Observer for Sensorless Control of PM Synchronous Motors With Online Parameter Identification", *IEEE Trans. on Ind. Electr.*, vol.: 60, Iss.: 2, 2013.

[13] G. Rinaldi , P. P. Menon, Ch. Edwards, A. Ferrara, "Sliding Mode Based Dynamic State Estimation for Synchronous Generators in Power Systems", *IEEE Control Systems Letters*, vol. 2, no. 4, October 2018.

[14] R. Kumar, S. Das, "MRAS-based speed estimation of grid-connected doubly fed induction machine drive," *IET Power Electron.*, vol. 10, no. 7, pp. 726–737, 2017.

[15] P. Pura, G. Iwanski, "Direct Torque Control of a Doubly-Fed Induction Generator Connected to Unbalanced Grid," *Polish Electrical Review*, vol. 1(5), 42–46, 2016. DOI: 10.15199/48.2016.05.08

[16] P. Xiong,D. Sun, D.,"Backstepping-Based DPC Strategy of a Wind Turbine-Driven DFIG under Normal and Harmonic Grid Voltage,"

IEEE Trans. on Power Electron, vol. 31(6), 4216–4225. DOI: 10.1109/TPEL.2015.2477442.
[17] J. Maneiro, R. Ryndzionek, T. Lagier, P. Dworakowski and C. Buttay, "Design of a SiC based triple active bridge ceil for a multi-megawatt DC-DC converter”, (EPE'17 ECCE Europe), 2017, pp. P.1-P.10, doi: 10.23919/EPE17ECCEEurope.2017.8099005.
[18] P. Vidal, M. Pietrzak-David, "Flux sliding mode control of a doubly fed induction machine," *Proc. of European Conference on Power Electronics and Applications*, Dresden, 2005, pp. 10 pp.-P.10. DOI: 10.1109/EPE.2005.219569.
[19] R. Ryndzionek, M. Michna, M. Ronkowski, J-F. Rouchon, „Analytical modelling of the multiceli piezoelectric motor based on three resonance actuators, IECON 2014, DOI: 10.1109/IECON.2014.7048888.

X. BIOGRAPHIES

Marcin Morawiec received the M.Sc. degree in electrical engineering from Czestochowa University of Technology, Czestochowa, Poland in 2003, Ph.D. degree from Gdansk University of Technology, Gdansk, Poland in 2007 and D. Sc. in 2017, IEEE Senior Member in 2020. Since 2017, he has been an Associate Professor in Gdansk University of Technology. He is author of over 95 articles and 2 monographs and 2 chapters in books, 1 Polish patent and 5 patent applications. His main scientific activities are concentrated on multi-scalar models, nonlinear control of any electrical machines, sensorless control, nonlinear control, backstepping control, adaptive observer backstepping and sliding mode control.

Krzysztof Blecharz Krzysztof Blecharz received the M.Sc. degree in electrical engineering from Czestochowa University of Technology, Czestochowa, Poland, in 2002 and the Ph.D. degree from Gdansk University of Technology, Gdansk, Poland, in 2008 in electrical drives. Since 2008, he has been an adjunct professor with Gdansk University of Technology. He is the author of over 15 articles, one Polish patent and a participant of many research projects as a designer or researcher. His main scientific activities are concentrated on doubly-fed generator control systems, multiscalar models of electrical machines, sensorless control, and nonlinear control in electric drives.

Arkadiusz Lewicki received the Ph.D. and D.Sc degrees in electrical drives from the Faculty of Electrical Engineering, Gdansk University of Technology, Gdansk, Poland in 2003 and 2013, respectively. He is currently with the Institute of Automatic Control of Electric Drives, Gdansk University of Technology. His scientific activities are concentrated on microprocessor control of converters, multilevel converters, pulse width modulation techniques, and nonlinear control of drives.